

Carbon isotope fractionation and depletion in TMC1¹

H. S. Liszt

National Radio Astronomy Observatory

520 Edgemont Road, Charlottesville, VA, 22903-2475

and

L. M. Ziurys

Arizona Radio Observatory

University of Arizona, 933 N. Cherry Avenue, Tucson, AZ 85721

hliszt@nrao.edu

Received _____; accepted _____

ABSTRACT

$^{12}\text{C}/^{13}\text{C}$ isotopologue abundance anomalies have long been predicted for gas-phase chemistry in molecules other than CO and have recently been observed in the Taurus molecular cloud in several species hosting more than one carbon atom, i.e. CCH, CCS, CCCS and HC_3N . Here we work to ascertain whether these isotopologic anomalies actually result from the predicted depletion of the $^{13}\text{C}^+$ ion in an oxygen-rich optically-shielded dense gas, or from some other more particular mechanism or mechanisms. We observed $\lambda 3\text{mm}$ emission from carbon, sulfur and nitrogen-bearing isotopologues of HNC, CS and H_2CS at three positions in Taurus (TMC1, L1527 and the NH_3 peak) using the ARO 12m telescope. We saw no evidence of $^{12}\text{C}/^{13}\text{C}$ anomalies in our observations. Although the pool of C^+ is likely to be depleted in ^{13}C , ^{13}C is not depleted in the general pool of carbon outside CO, which probably exists mostly in the form of C^0 . The observed isotopologic abundance anomalies are peculiar to those species in which they are found.

Subject headings: astrochemistry . ISM: molecules . ISM: clouds. Galaxy

1. Introduction

Observations of isotopically-substituted versions of interstellar molecules – their so-called isotopologues – have become the usual way of deducing atomic isotopic abundance ratios for common products of stellar nucleosynthesis – C, N, O, S, Si, Cl etc in the interstellar medium (ISM), as summarized by Wannier (1980) and Wilson (1999). However, the relative abundances of particular isotopologues can differ from those inherent in the gas at large owing to peculiarities of their chemistry (Watson et al. 1976; Watson 1977; Langer et al. 1984), and recognizing or explaining anomalous isotopologic abundance ratios is an ongoing challenge for astrochemistry.

The most commonly-observed example of this phenomenon is with CO in diffuse clouds, where the the CO/ ^{13}CO ratio may be larger or smaller than the inherent C/ ^{13}C ratio in the ambient gas depending on whether selective photodissociation (Bally & Langer 1982) or chemical fractionation (Watson et al. 1976)) dominates (Wilson et al. 1992; Liszt & Lucas 1998; Sonnentrucker et al. 2007; Burgh et al. 2007; Sheffer et al. 2008; Liszt 2007; Visser et al. 2009). Selective photodissociation (increasing CO/ ^{13}CO) occurs in gas seen toward a few hot stars while chemical fractionation (behaving oppositely) is a more general phenomenon that is enhanced at somewhat higher CO column densities. Chemical fractionation is also now seen in the envelopes of dark clouds (Goldsmith et al. 2008).

Gas-phase molecular cloud chemistry actually makes a rather general prediction about isotopologic abundances in strongly shielded regions: CO and molecules that form directly from it (HCO^+ , H_2CO and CH_3OH) should show a common C/ ^{13}C ratio that reflects the composition of the gas reservoir, while other species that form from the pool of free carbon outside CO should be strongly depleted in ^{13}C (Watson 1977; Liszt 1978; Langer et al. 1984). This occurs

¹Based on observations obtained with the ARO Kitt Peak 12m telescope.

because CO is the repository of the overwhelming majority of the gas-phase carbon² and carbon is liberated from CO mainly as the dissociation product of destruction of CO by a small quantity of cosmic-ray ionized He⁺ (i.e. $\text{He}^+ + \text{CO} \rightarrow \text{C}^+ + \text{O} + \text{He}$). The resulting C⁺ ions quickly interact with the ambient CO, and the fact that ¹³CO is more strongly bound than ¹²CO results in a preferential deposition of ¹³C into ¹³CO through the reaction $^{13}\text{C}^+ + ^{12}\text{CO} \rightarrow ^{12}\text{C}^+ + ^{13}\text{CO} + 34.8$ K (Watson et al. (1976), see Appendix A here). In this way ¹³C⁺ preferentially disappears from the pool of C⁺ and from the general pool of carbon available to form most species. The C⁺/¹³C⁺ ratio increases by a factor approaching $\exp(34.8/T_K)$ but the CO/¹³CO ratio changes little because the C⁺/CO abundance ratio is so small, below 10⁻³.

It quickly became apparent that there was some tension between this prediction and observations of interstellar gas showing C/¹³C ratios that were, if anything, *below* the terrestrial value of C/¹³C = 89. Now it is acknowledged that the local interstellar carbon isotope ratio is in the range 60-70, but at the time, Watson (1977) suggested a mechanism involving selective depletion of carbon onto grains, offering the possibility of lowering the C/¹³C ratio. Detailed time-dependent models showed very complex behaviour in the isotopologic ratios but largely failed to bear out this suggestion (Liszt 1978), finding that ¹³C enhancement outside CO only occurred as molecules disappeared from the gas.

Because of the possibility of fractionation in fully molecular gas, some observers changed the focus of their work to concentrate on measurement of carbon isotope ratios using only the isotopologues of carbon monoxide (Langer & Penzias 1993) but it seems fair to say that anomalously large C/¹³C ratios have never been seen in the molecular cloud-H II region complexes that are typically used for isotope determinations (Wannier 1980; Wilson 1999). Indeed, a recent survey of the carbon isotope ratio in CN does not seem to have been affected (Milam et al. 2005) and Tercero et al. (2010) report C/¹³C = 45 ± 20, S/³⁴S = 20 ± 6 from a survey of sulfur-bearing

²at least as long as [O] > [C]

carbon chain molecules in Ori KL. Fractionation effects may be minimized at the somewhat higher temperatures of clouds near H II regions but are not entirely eliminated. The absence of observable effects from the predicted carbon fractionation chemistry has been a lingering, if not entirely obvious, mystery.

By contrast, anomalies of two kinds have now been noted in cold gas in/near the cyanopolyne peak in the Taurus Molecular Cloud (TMC) for species containing several carbon atoms, and Sakai et al. (2007) and Sakai et al. (2010) appealed to the work of Langer et al. (1984) for an explanation. ^{13}C is strongly but very unequally lacking in both of the singly-substituted ^{13}C isotopologues of CCH (Sakai et al. 2010) and is deficient in ^{13}CCS but not C^{13}CS . A small effect may also be present in HC_3N in Taurus (Takano et al. 1998) and Martín et al. (2010) recently reported $\text{N}(\text{CCH})/\text{N}(^{13}\text{CCH}) > 110$ (3σ) in M 82.

The gas-phase carbon isotopic chemistry is the subject of this work. Motivated by the apparent contradictions among the model predictions for a strong depletion of ^{13}C , the absence of any obvious effect in subsequent measurements like those reported by Milam et al. (2005) for CN and ^{13}CN , and the recent invocation of a general ^{13}C depletion to explain anomalies seen in the nearby Taurus Cloud (Sakai et al. 2007, 2010), we observed isotopologues of species containing a single carbon (CS, HNC and H_2CS) toward three positions in Taurus, as described in Sect. 2. Section 3 summarizes the observational situation including our new measurements. Having found no evidence that ^{13}C is depleted in the species we observed, and probably in the general pool of carbon in the gas, we discuss the overall carbon chemistry in Sect. 4, inquiring how ^{13}C depletion can be *avoided* and the implications for the gas phase chemistry if it does *not* actually occur.

2. Observations and conventions

The new observations reported here were taken at the ARO 12m telescope in 2011 March and April. We observed HNC, CS, H₂CS and their singly-substituted ¹³C, ¹⁵N and ³⁴S isotopologues at three positions in Taurus: the TMC1 cyanopolyynes peak ($\alpha = 4^{\text{h}}41^{\text{m}}42.88^{\text{s}}$, $\delta=25^{\circ}41'27''$), L1527 ($\alpha = 4^{\text{h}}39^{\text{m}}53.89^{\text{s}}$, $\delta=26^{\circ}03'11''$) and the NH₃ peak ($\alpha = 4^{\text{h}}41^{\text{m}}23^{\text{s}}$, $\delta=25^{\circ}48'13.3''$; all coordinates are J2000). All the data were taken by position-switching to an off-position 8.5' NE of the cyanopolyynes peak, using the dual-polarization mode of the autocorrelator configured for 24.4 kHz channel spacing (0.073 km s⁻¹ at 100 GHz) and 48.8 kHz spectral resolution. Typical system temperatures were 180 - 240 K depending on line frequency and source elevation. All velocities are given with respect to the kinematic local standard of rest and the line temperatures are given in terms of the native scale at the ARO 12m, $T_{\text{R}}^* \approx 0.85 T_{\text{mb}}$. Line frequencies were taken from the online splatalog (<http://www.splatalogue.net>) and are given in Table 1 representing the new results.

In this work we do not call out the most-abundant isotope explicitly: C implies ¹²C. The integrated intensity of spectral lines for species X, in units of K km s⁻¹, is denoted by W(X).

3. Observational results

3.1. New results

Spectra are shown in Fig. 1 and numerical results are summarized in Table 1 giving profile integrals and Table 2 giving ratios of line profile integrals and implied carbon isotope ratios, assuming values for N/¹⁵N or S/³⁴S as indicated.

The main isotopologues of HNC and CS are optically thick and self-absorbed by weakly-excited molecules within the foreground envelopes; it is not possible to measure the C/¹³C ratios

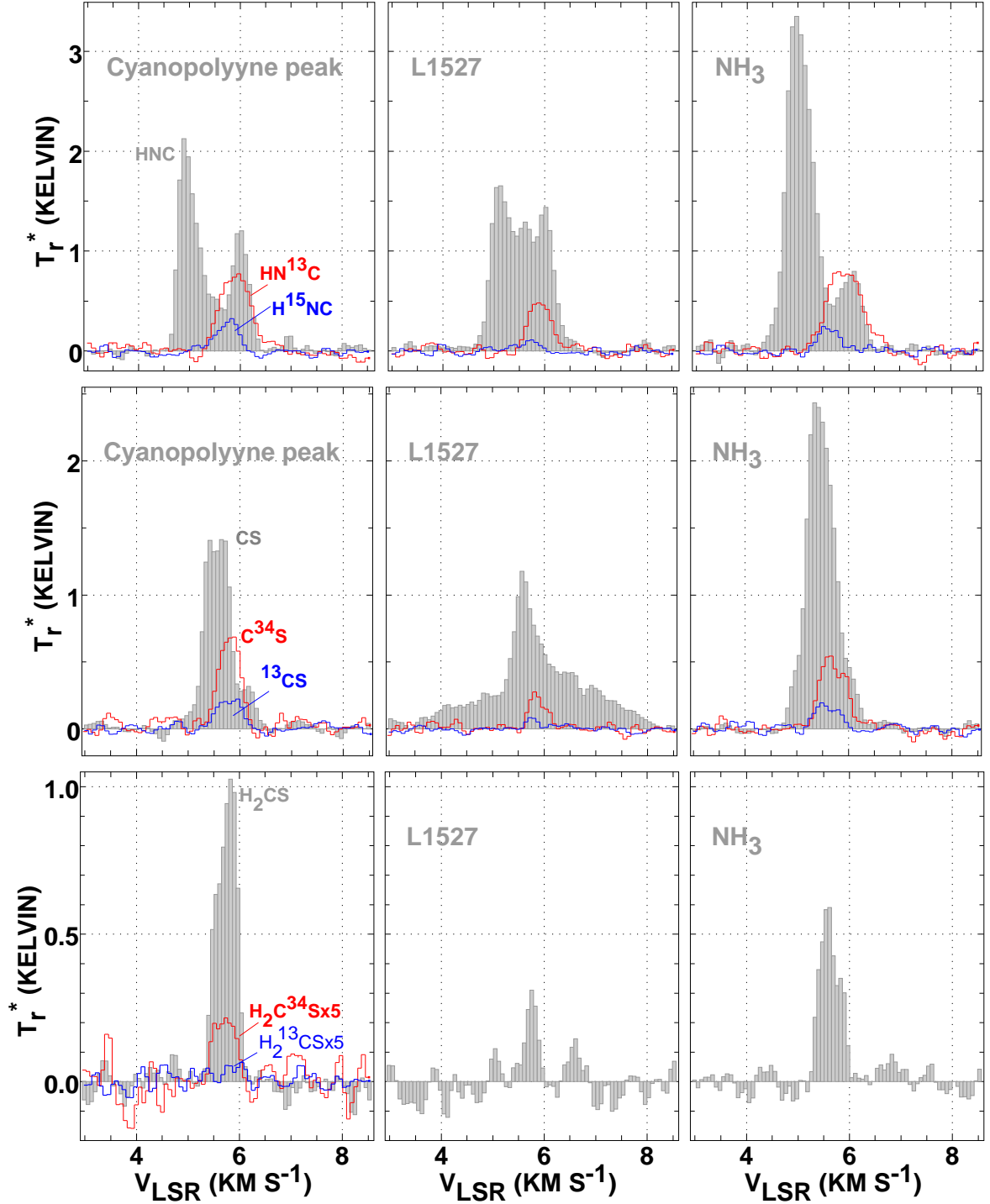


Fig. 1.— Observed line profiles toward three positions in TMC1

in these species directly and we must assume values for the isotopologic ratios in sulfur and nitrogen. For nitrogen the interstellar $N/^{15}N$ ratio is now seen to be only slightly larger than the terrestrial ratio of 270. Lis et al. (2010) found $N/^{15}N = 334 \pm 50$ (3σ) toward Barnard 1 and Adande and Ziurys (in press) find $N/^{15}N = 290 \pm 40$ at the Solar Circle from a large-scale galactic survey of CN emission. In local diffuse clouds Lucas & Liszt (1998) found $N/^{15}N = 240 \pm 25$. The range of values implied for $HNC/HN^{13}C$ in Table 2 corresponds to $HNC/H^{15}NC = 250$ -330 and the statistical uncertainties are quoted at each end of the range.

No systematic deviations from the Solar System value of $S/^{34}S = 22.7$ have been seen in specific isotope studies of the local ISM (Wannier 1980; Wilson 1999; Tercero et al. 2010) and the implied values of $CS/^{13}CS$ quoted in Table 2 correspond to this value and the statistical uncertainties of the current measurements. Our measurements of H_2CS isotopologues toward TMC1 are in accord with this. Some uncertainty accrues from the unmeasured optical depth of the rarer isotopologic lines as discussed in the following subsection.

The result for the isotopologic carbon ratio in H_2CS is of marginal significance and will not be discussed further but it seems clear from Table 2 that there is no strong depletion of ^{13}C in HNC or CS.

3.2. Correction for finite optical depth

3.2.1. CS

The presence of a finite optical depth in the $C^{34}S$ line would cause compression of the $W(C^{34}S)/W(^{13}CS)$ intensity ratio, resulting in an underestimate of the $N(C^{34}S)/N(^{13}CS)$ and $N(CS)/N(^{13}CS)$ column density ratios. For TMC1, Pratap et al. (1997) derived $N(C^{34}S) = 2.0 \times 10^{12} \text{ cm}^{-2}$, consistent with an estimate $N(C^{34}S) = N(CS)/22.7 = 5 \times 10^{13} \text{ cm}^{-2}/22.7 = 2.2 \times 10^{12} \text{ cm}^{-2}$ from the work of Ohishi et al. (1992). For $N(C^{34}S) = 2.0 \times 10^{12} \text{ cm}^{-2}$ and peak line

brightness of 0.72 K - 0.85 K, depending on beam efficiency, we calculate that the central optical depth of the C^{34}S $J=2-1$ line toward TMC1 must be below 0.15 and the excitation temperature in the lower part of the rotation ladder must be fairly high, above about 8 K for $J=2-1$, based on modelling of the excitation. In this case the ^{13}CS line is quite optically thin and the observed isotopologic intensity ratio is at most 5% below the intrinsic abundance ratio. Accordingly, the entry corrected for optical depth in Table 2 is the uncorrected value increased by 5%.

Estimates of the optical depth correction toward the other pointing positions do not seem possible. Toward the NH_3 peak Pratap et al. (1997) derived a higher column density $N(\text{C}^{34}\text{S}) = 4.3 \times 10^{12} \text{ cm}^{-2}$ while the observed line in this work is only slightly broader and noticeably less bright. Excitation solutions for such high column density in the face of relatively weak emission indicate high optical depth at lower excitation temperatures (5 K) that do not seem consistent with the physical conditions toward the NH_3 peak, that are not less dense or colder than toward TMC1. Pratap et al. (1997) cited problems with their modelling of the CS lines, such that they were compelled to use a very small isotopologic abundance ratio $\text{CS}/\text{C}^{34}\text{S} = 12-14$. Although they cited a reference to the isotopic composition of cosmic rays in defense of this assumption, it is without precedent in molecular gas and would lead to improbably small values of the $\text{CS}/^{13}\text{CS}$ ratio if used in this work. We conclude that we cannot make a reliable correction for optical depth correction except toward TMC1 where all indications are that the opacities in the rarer CS isotopologues are small.

3.2.2. *HNC*

For HNC, the ^{13}C -bearing isotopologue is the more abundant of the two variants used to derive the $\text{C}/^{13}\text{C}$ ratio, so the effect of optical depth is opposite to that in the case of CS: the derived $\text{HNC}/\text{HN}^{13}\text{C}$ ratio decreases with increasing optical depth in the rare isotopologues. Indeed, the optical depths encountered in HNC are higher than for CS and the correction for

finite optical depth is rather larger. Unfortunately we did not resolve the hyperfine structure of HN^{13}C and cannot duplicate the excitation temperature/opacity derivation of Padovani et al. (2011) who observed at other positions in Taurus having higher optical depth than occurs toward TMC1.

Pratap et al. (1997) gave $N(\text{HN}^{13}\text{C}) = 4.2 \times 10^{12} \text{ cm}^{-2}$ toward TMC1 while a slightly smaller upper limit $N(\text{HN}^{13}\text{C}) < 2 \times 10^{14} \text{ cm}^{-2}/60 < 3.3 \times 10^{12} \text{ cm}^{-2}$ can be inferred from the tabulation of Ohishi et al. (1992). For the comparatively weak emission lines we observed, these column densities imply $J=1-0$ excitation temperatures around 4 K and optical depths of order 2 in HN^{13}C , so that even such a rare isotopologue would be somewhat self-absorbed. With optical depths this large, simply requiring that $\text{HNC}/\text{HN}^{13}\text{C}$ be above 60 limits the possible range of assumed values for $N(\text{HNC})/N(\text{H}^{15}\text{NC})$ to be nearer the large end of the likely range. However, the small excitation temperatures implied by our observed brightnesses and the higher of the previously measured column densities are not consistent with the densities that are inferred for the Taurus cores, which imply higher excitation temperatures, lower optical depths and smaller column densities.

We conclude that it is not possible to derive an entirely accurate carbon isotopologue ratio in HNC based on correcting the observed intensity ratios for optical depth but the errors do go in a known direction. Table 2 shows a range of carbon isotope ratios derived from HNC for an optical depth 0.6 in the HN^{13}C line toward TMC1, corresponding to an excitation solution with $N(\text{HN}^{13}\text{C}) = 2 \times 10^{12} \text{ cm}^{-2}$ that is consistent with the work of Ohishi et al. (1992). This could still underestimate the optical depths and so overestimate the $\text{C}/^{13}\text{C}$ ratio.

3.3. Previously-reported ^{13}C anomalies

These are summarized in Table 3 where all the results are cast in terms of actual or implied $\text{C}/^{13}\text{C}$ ratios, using the terrestrial sulfur isotopic ratio as appropriate. There are two effects

that must be considered: ^{13}C is strongly lacking in some isotopologues but to different degrees depending upon placement. Thus both ^{13}CCH and C^{13}CH are underabundant but moreso in the former (a factor 1.6) and in CCS only the more tightly-bound isotopologue ^{13}CCS exhibits the effect; in each case, the isotopologue with an inboard ^{13}C is more abundant. In C_3S only $^{13}\text{CCCS}$ was observed, but is heavily deficient. In terms of chemical models these two considerations are separately reflected in, on the one hand, the overall $\text{C}/^{13}\text{C}$ ratio in the gas, and, on the other, the detailed path to formation (and perhaps in situ fractionation after formation) of the individual species studied.

Sakai et al. (2007) and Sakai et al. (2010) discussed in exquisite detail the formation routes to CCS and CCH, concluding that the unequal depletions of the ^{13}C -bearing isotopologues were the result of formation reactions in which the carbon atoms were not equivalent (for CCH, $\text{C} + \text{CH}_2 \rightarrow \text{CCH} + \text{H}$ and not $\text{C}_2\text{H}_3^+ + \text{e} \rightarrow \text{CCH} + \text{H}_2$), rather than alterations that might have occurred after formation (for instance $^{13}\text{CCH} + \text{H} \rightarrow \text{C}^{13}\text{CH} + \text{H} + 8.1 \text{ K}$ or $^{13}\text{CCS} + \text{S} \rightarrow \text{C}^{13}\text{CS} + \text{S} + 15 \text{ K}$). They also concluded that they had confirmed observationally the phenomena modelled by Langer et al. (1984) whereby the relatively famous fractionation reaction involving CO and C^+ induces a very general vanishing of ^{13}C from the gas at large as discussed in the Introduction here.

4. Carbon isotopic and isotopologic ratios in the Taurus cores

The $\text{C}/^{13}\text{C}$ ratios inferred from our work are consistent with other measurements of the carbon isotopic ratio in the nearby ISM that find $\text{C}/^{13}\text{C} = 60\text{-}70$ and show no sign of the ^{13}C depletion that is predicted for the gas phase chemistry. The CS isotopologues we observed would not serve as the basis for substantially depleted CCS but are instead close to the $\text{CCS}/\text{C}^{13}\text{CS}$ ratio 54 ± 2 discussed by Sakai et al. (2007), suggesting that CCS could indeed form directly through a reaction like $\text{CH} + \text{CS} \rightarrow \text{CCS} + \text{H}$ as hypothesized by Sakai et al. (2007).

In fact, Furuya et al. (2011) recently reached something of the same conclusion through chemical modelling, without the new observational result for CS. They considered a time-dependent model for TMC1 with all the carbon initially in the form of C^+ (see Liszt (2009)), in which the abundance of CO is relatively small even when it begins to deplete out of the gas onto grains; the CO column in their model is also rather small compared with $N(CO) = 500 N(C^{18}O) = 1.8 \times 10^{18} \text{ cm}^{-2}$ from Pratap et al. (1997). Because of the assumed initial conditions a very large proportion of the gas-phase carbon remains outside CO, and, for reasons that are discussed in Sect. 5, ^{13}C depletion in the gas as a whole is generally modest. $C/^{13}C$ is typically of order 110 after the earliest times. In this case the hypothesis of a rearrangement effected by reaction of CCS and H yielded $CCS/^{13}CCS = 230$, $CCS/C^{13}CS = 54$, as observed. That is, the rare isotopologues both form with $C/^{13}C = 110$ but the hypothesized reaction $C^{13}CS + H \rightarrow ^{13}CCS + 17.4 \text{ K}$ is strongly energetically favored at 10 K driving $CCS/^{13}CCS$ up while $CCS/C^{13}CS$ falls to half the $C/^{13}C$ ratio in the gas (110/2). Our results suggest that ^{13}CCS and $C^{13}CS$ actually form with $CCS/^{13}CCS$ and $CCS/C^{13}CS \approx 70$.

Furuya et al. (2011) also showed that the known rearrangement reaction for CCH with ambient H (that has a smaller exothermicity 8 K) could yield unequal isotopologic abundances to the degree observed (a factor 250/170) but the relatively small amount of ^{13}C depletion in their model did not come close to reproducing the very large individual $CCH/^{13}CCH$ or $CCH/C^{13}CH$ ratios that are observed (170 and 250; Table 3). Even so, their model generally predicts larger values for $N(CS)/N(^{13}CS)$ than we observe. It is not obvious that this scheme would function as well in a gas that was even more weakly fractionated, if it caused very small values for the $CCS/^{13}CCS$ ratio.

The smaller isotopologic discrepancies that are observed in HC_3N can likely be achieved by relatively weakly-endothermic rearrangement reactions with hydrogen in an unfractionated gas, consistent with the lack of fractionation we infer for HNC. In summary, the observational

situation is complex and somewhat mysterious. CS, HNC and HC₃N suggest that there is little fractionation in the carbon pool at large while the seeming absence of fractionation in CCS/C¹³CS may be accidental and the anomalies in CCH remain unexplained. Disparities among the carbon isotopologues in individual species with more than one carbon atom seem best explained by rearrangement reactions with atomic hydrogen but the very large isotopologic ratios seen in CCH remain beyond the reach of current explanations and the disparity that is observed in CCS may be inconsistent with rearrangement in a gas that is too-lightly fractionated.

5. Where is the CR ionization-driven fractionation?

The possibility of a strong overall carbon fractionation in species other than CO has been recognized ever since the existence of the C⁺ + CO fractionation reaction was first remarked. Nonetheless, it was not observed in surveys that sought to determine the carbon isotope ratio but found the same values in CO and CS and CN etc, even though the latter species do not form from CO and could have shown strong fractionation effects even in relatively warm gas. Even now, despite the carbon isotopologic anomalies that are seen at very low temperatures (10 K) in Taurus in some polyatomics bearing more than one carbon, the gas there can not obviously be said to be fractionated as a whole. Here we ask why this is so.

5.1. The role of He⁺

The prediction of strong overall fractionation arises in models of the gas-phase chemistry of dense dark oxygen-rich material (O/C > 1) where CO is by far the largest repository of gas-phase carbon atoms (Langer et al. 1984). A few molecular species form directly from CO – HCO⁺ in the gas, H₂CO and CH₃OH from successive hydrogenation of CO on grains – and will share its C/¹³C ratio. Other carbon-bearing trace molecules in the gas result from the relatively small amount of

carbon that is liberated when He^+ , ionized by cosmic rays, slices CO apart into C^+ and O via the reaction $\text{He}^+ + \text{CO} \rightarrow \text{C}^+ + \text{O} + \text{He}$; the reaction rate constant is $1.6 \times 10^{-9} \text{ cm}^3 \text{ s}^{-1}$ (see Table 4 for important reactions and rate constants). The only reaction competing effectively with this one for the attentions of He^+ is the charge-exchange ionization of H_2 , $\text{He}^+ + \text{H}_2 \rightarrow \text{He} + \text{H}_2^+$, whose currently-accepted reaction rate constant is $7.2 \times 10^{-15} \text{ cm}^3 \text{ s}^{-1}$ (Table 4). Langer et al. (1984) included instead the reaction $\text{He}^+ + \text{H}_2 \rightarrow \text{H}^+ + \text{H} + \text{He}$ with the much larger rate constant $1.5 \times 10^{-13} \text{ cm}^3 \text{ s}^{-1}$, which significantly dampened the effects of fractionation compared to what would be derived in more recent chemical models: that reaction is now considered to be negligibly slow in cold gas, see Table 4.

The ratio of reaction rates and abundances determines whether CO or H_2 controls the abundance of He^+ but for $X(\text{CO}) > 4.5 \times 10^{-6}$, when CO dominates using currently-accepted reaction rate constants, every cosmic-ray ionization of an He atom results in the production of a C^+ ion. Because He is so much more abundant than carbon (i.e. CO), the volume rate of production of C^+ ions and the rate at which carbon is liberated from CO is approximately 1000 times higher than the rate at which cosmic rays interact with CO directly; this factor is independent of the cosmic ray ionization rate $n(\text{He}^+)$ and independent of $X(\text{CO})$ when the reaction with CO is the main destroyer of He^+ .

It is important to stress just how rapidly the chemical ionization of carbon occurs via $\text{He}^+ + \text{CO}$, because the only competing mechanism for liberating atomic carbon from CO is photodissociation. In quiescent, shielded, cosmic-ray heated gas, cosmic-ray induced photodissociation typically occurs at rates that are a much smaller multiple of the cosmic ray ionization rate, and is some 50 times slower than $\text{He}^+ + \text{CO}$. The point is that in these models it is difficult to contrive to liberate carbon from CO except, initially, as C^+ , leading to fractionation.

5.2. The role of the CO + C⁺ fractionation reaction

Just as He⁺ reacts most commonly with CO, so does C⁺, although in this case there is a wider range of competitive reactions (see Table 4). But to the extent that C⁺ interacts with CO, it preferentially deposits ¹³C⁺ back in CO. Meanwhile, the abundance of C⁺ is so small relative to that of CO (typically less than 0.1%) that any effect on the isotopologic abundance ratio in CO is imperceptible. The final result is that when free atomic carbon is primarily liberated and maintained in the form of C⁺, the pool of gas-phase carbon outside CO inevitably becomes depleted in ¹³C⁺, hence in ¹³C, as long as CO remains sufficiently abundant in the gas to dominate the neutralization of He⁺. CO and the free carbon pool coexist but with two distinct C/¹³C ratios that are separately passed on to their descendant molecules.

5.3. So indeed, why is a more general ¹³C depletion not seen in Taurus?

To blunt the effect of C⁺ fractionation it is necessary to interfere with the C⁺-CO interaction and there are various choices for doing so, for instance; i) a low CO abundance, such as might occur at later times after depletion onto dust (see also the early-time model of Furuya et al. (2011) in which CO never attains its full abundance); ii) very large abundances of species like OH and O₂ that react rapidly with C⁺; iii) taking the high-metals case where sulfur and silicon are not assumed to be strongly depleted from the gas so that they dominate the neutralization of C⁺ through charge exchange; iv) the presence of PAH (Wakelam & Herbst 2008; Lepp et al. 1988) to neutralize C⁺ more rapidly, although these are not always assumed to survive in dense gas. Nonetheless, fractionation at the level of a factor two or so persists in the C⁺ until CO and C⁺ are all but gone from the gas.

Preventing fractionation of the pool of molecules outside the small family that forms from CO really requires that the reservoir of carbon outside CO must reside mostly in the form of

neutral atomic carbon with perhaps some small admixture of C^+ . Given that C^0 typically reacts with neutral molecules at least 20 times more slowly than does C^+ , the proportion of C^0 to C^+ should be very large and the real question is how this might come about. One possibility that is capable of maintaining very large free neutral atomic carbon fractions is the so-called high ionization phase of bistable solutions of the chemical equilibrium equations, whose relevance has recently been discussed in terms remarkably similar to the considerations here for controlling the C^+ abundance (Charnley & Markwick 2003; Wakelam et al. 2006; Boger & Sternberg 2006). Extension of the bistability discussion to include fractionation effects is clearly of great interest.

It is generally *not* possible to create a sufficient pool of neutral carbon using just the in situ flux of CO-dissociating photons generated by the cosmic ray-induced electronic excitation of H_2 (Prasad & Tarafdar 1983; Sternberg et al. 1987) because these photons dissociate CO at rates that are a relatively small multiple of the cosmic ray ionization rate: Langer et al. (1984) assumed a multiple of 10. As such, cosmic-ray induced photons liberate neutral atomic carbon much more slowly than CO is sliced into C^+ and O by He^+ . Because the naturally-arising local flux of CO photodissociating photons inside dark gas is so weak, some attempts to explain the existence of even a relatively small amount of C^0 in dense gas invoke special mechanisms such as inversion of the normal $[O]/[C] > 1$ ratio (Langer et al. 1984), penetration of ambient uv light into a porous, heavily clumped medium and/or recent cloud formation (Phillips & Huggins 1981), turbulent diffusion that cyclically exposes heavily-shielded gas to the ambient uv radiation field near the cloud surface (Boland & de Jong 1982; Willacy et al. 2002; Xie et al. 1995) and the presence of the so-called high-ionization phase of bistable chemical reaction schemes (Flower et al. 1994).

The inference of a large pool of free atomic carbon in dense dark gas is really not an observational problem per se because substantial columns of C^0 are typically found toward and around dark clouds (Frerking et al. 1989) including toward TMC1 where $N(C^0)/N(CO) \simeq 0.1$ (Maezawa et al. 1999). This is very large compared to the values $X(C^+)/X(CO)$

$\sim 3 \times 10^{-8} / 8 \times 10^{-5} \sim 4 \times 10^{-4}$ that arise from the default parameters in our toy model (Appendix B). However, the observational situation is complicated by superposition of different density regimes along the line of sight and it is hard to assess how much of the observed atomic carbon actually exists inside the darkest gas. This is especially true given the recent revelation of the preponderance of low- A_V material in Taurus and other dark cloud complexes (Pineda et al. 2010; Cambr  s 1999). Extrapolation of the results of Bensch et al. (2003) to much higher $N(\text{CO})$ suggests that perhaps 1-2% of the carbon budget (Gerin et al. 2003) could exist as C^0 at $N(\text{CO}) \approx 10^{18} \text{ cm}^{-2}$. This would be about 50 times more carbon than exists in C^+ .

5.4. Relevance to other environments

The possibility of chemical fractionation in cold cores raises important questions for understanding carbon isotopic abundances in planetary and proto-planetary systems including the Solar System and proto-Solar nebula. For example, is it correct to ascribe the difference between the Solar ratio $\text{C}/^{13}\text{C} = 89$ and that in the nearby ISM (60-70) entirely to chemical enrichment since the birth of the Solar System or might fractionation be responsible (Smith et al. 2011) ? Why are there differences between the carbon isotope ratios measured in various comets and between those measured in comets and that in the Sun (Crovisier et al. 2009; Mumma & Charnley 2011). Other questions arise in matters involving other elements, for instance the difference between the $\text{N}/^{15}\text{N}$ ratio in the Earth (270) and Sun (420) and the wide disparities in D/H measurements between that in the earth’s oceans (1.6×10^{-4}), the more nearly cosmological ratios seen in the outer planets ($3 - 5 \times 10^{-5}$) and the much higher than telluric D/H ratios seen in most comets (Crovisier et al. 2009; Mumma & Charnley 2011), although, apparently, not all (Hartogh et al. 2011).

Many of the effects discussed here occur prominently in recent models of fractionation chemistry in protoplanetary disks (Woods & Willacy 2009), which illustrate the complexity of

relating isotope ratios in the proto-planetary nebula or planetary disk (when formed) to that in the ambient natal material. Fractionation varies with disk radius and disk height and evolves with time under the combined influence of the proto-stellar and interstellar radiation fields. Woods & Willacy (2009) conclude that Solar System cometary material has been reprocessed, raising the question of whether any memory of conditions in natal molecular material persists into fully-formed planetary systems.

6. Summary

Since the initial recognition of the carbon isotope fractionation reaction a conflict has existed between the very general prediction of a strong ^{13}C depletion in molecules other than CO and the general absence of observable effects in surveys of the $\text{C}/^{13}\text{C}$ isotopic abundance ratio deduced from such common species as CS or CN. ^{13}C depletion is predicted to occur when carbon is liberated from CO by the reaction $\text{He}^+ + \text{CO} \rightarrow \text{C}^+ + \text{O} + \text{He}$ and remains in the gas as C^+ to interact and fractionate with CO. Eventually, CO depletion onto grains will blunt the effect at late times but in the meanwhile quite large variations in the abundances of ^{13}C -bearing molecules are predicted for all species that do not form directly from CO. The point is that CO remains very nearly unfractionated as long as it is the main carbon reservoir in the gas and $\text{X}(\text{C}^+)/\text{X}(\text{CO})$ is very small, so that species like HCO^+ , H_2CO and CH_3OH will also be unfractionated. But the relatively small pool of carbon that exists outside of CO to form other molecules than those in the CO family becomes strongly depleted in $^{13}\text{C}^+$ and molecules that form from it (most carbon-bearing species) will also show strong ^{13}C depletion.

However, strong anomalies in CCH and in some isotopologues of CCS and CCCS have recently been observed in cold dark gas in TMC1 and other cores in Taurus (less strongly in HC_3N there). It was suggested that the predicted fractionation effects had at long last actually been seen, albeit in only some very cold gas. We showed here that ^{13}C fractionation does not occur in two

species having a single carbon (CS and HNC) seen toward TMC1 in Taurus; we also observed these species toward other positions, finding certainly no clear evidence of fractionation, but derivation of an accurate isotopic abundance was frustrated by the difficulty of correcting for finite optical depth even in very rare isotopologues. In any case, our observations toward TMC1 make it unlikely that any general depletion of ^{13}C exists in the gas at large outside CO and we discussed the implications of this inference in the context of the chemistry of an optically shielded dense gas with a normal ratio $[\text{O}]/[\text{C}] > 1$.

In general, preventing an overall ^{13}C fractionation requires that the pool of gas-phase carbon outside CO resides in the gas mostly as C^0 rather than C^+ . This could happen if the $[\text{O}]/[\text{C}]$ ratio is less than unity or if some mechanism is invoked to liberate neutral carbon from CO through photodissociation deep inside dark gas but the most interesting possibility is that the TMC1 gas is in the so-called high ionization state of a bistable chemical network. In any case, we are left with the fact that the overall carbon pool outside CO is apparently not depleted in ^{13}C even if there is no way to prevent $^{12}\text{C}^+ / ^{13}\text{C}^+ \gg 60$. For the chemistry this has interesting consequences; reactions involving C^+ see a pool of carbon depleted in ^{13}C while those with C^0 do not, and the main pool of carbon is in larger amounts of C^0 that react somewhat more slowly, with a normal $^{12}\text{C}/^{13}\text{C}$ ratio.

In the future it may be possible to ascertain the overall composition of the carbon pool deep inside TMC1 using high spatial resolution observations of sub-mm lines of C I at ALMA, and perhaps even to measure the $\text{C}/^{13}\text{C}$ ratio using the 492.164 GHz line of ^{13}C that is displaced from the main isotope. In the meantime it is important to assess just which chemical species are subject to isotopologic abundance anomalies - apparently, a wide variety of tri- and polyatomics hosting more than one carbon atom – and under what conditions they arise, and to avoid using strongly affected molecules to derive isotopic abundance ratios.

The Arizona Radio Observatory is operated by Steward Observatory, University of Arizona, with partial support through the NSF ATI program. The National Radio Astronomy Observatory

is operated by Associated Universities, Inc. under a cooperative agreement with the US National Science Foundation. HSL wishes to acknowledge the hospitality of Gasthaus Leykauf in Rottach-Egern during the completion of the initial draft of this work and that of Bel Esperance in Geneva during the next. We thank the referee for a close reading of the manuscript and a variety of interesting suggestions for further discussion.

Facilities: ARO

A. Appendix A. The fractionation reaction

Smith & Adams (1980) did not give analytic forms for their measurements of the temperature dependence of the carbon fractionation reaction first cited by Watson et al. (1976). Liszt (2007) provided the expressions

$$k_f = 7.64 \times 10^{-9} T_K^{-0.55} \text{ cm}^3 \text{ s}^{-1} \quad (T_K = 80 - 500\text{K})$$

$$k_f = \frac{1.39 \times 10^{-9} T_K^{-0.05} \text{ cm}^3 \text{ s}^{-1}}{1 + \exp(-34.8/T_K)} \quad (T_K = 10 - 80\text{K})$$

$$k_r = k_f \exp(-34.8/T_K)$$

for the forward (exothermic) and reverse reaction rates k_f and k_r .

B. Appendix B. A toy model of ^{13}C depletion

We constructed a formal model of the chemistry in which C^+ is produced by the action of He^+ on a fixed abundance of CO ($X(\text{CO}) = n(\text{CO})/n(\text{H}_2)$ is a parameter) and solved for the densities

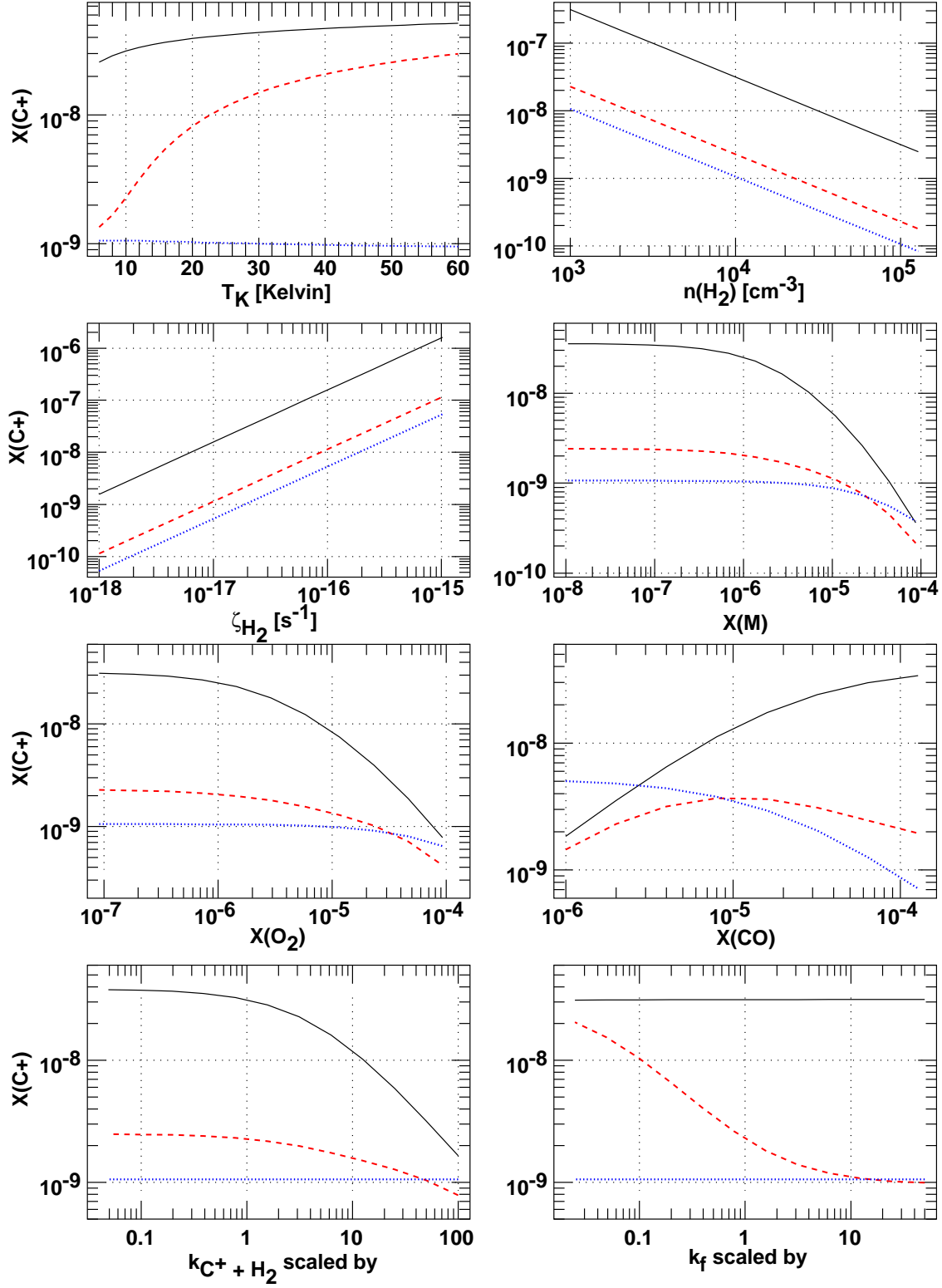


Fig. 2.— Toy model of the $^{13}\text{C}^+$, $^{12}\text{C}^+$ chemistry. In each panel the solid line is $X(\text{C}^+)$, the (red) dashed line is $[\text{C}^{12}]/[\text{C}^{13}] \times X(^{13}\text{CO})/X(^{12}\text{CO})$ and the (blue) dotted line is $X(\text{He}^+)$ (only shown in some panels). Standard values are $T_K = 10 \text{ K}$, $n(\text{H}_2) = 10^4 \text{ cm}^{-3}$, $\zeta = 2 \times 10^{-17} \text{ per H}_2$, $X(\text{CO}) = 8 \times 10^{-5}$, $X(\text{M}) = 3 \times 10^{-7}$, $X(\text{O}_2) = 3 \times 10^{-7}$ and $^{12}\text{C}/^{13}\text{C} = 60$. The panels of this figure show the

$n(^{12}\text{C}^+)$, $n(^{13}\text{C}^+)$ and $n(\text{He}^+)$. In addition to the fractionation reaction with CO, C^+ is destroyed by interaction with H_2 , hydrides (CH, NH, OH), O_2 , thermal electrons, and charge exchange with a single low-ionization metal species denoted “M” and given the atomic properties of silicon. For the reactions in Table 4 we used the dipole-enhanced rates given on the UFDA06 database website <http://www.udfa.net/> (Woodall et al. 2007).

The default values of the reactant abundances are given in Table 4 and quoted in Figure 2, i.e. $n(\text{H}_2) = 10^4 \text{ cm}^{-3}$, $T_K = 10 \text{ K}$, $\zeta_{\text{H}_2} = 2 \times 10^{-17} \text{ s}^{-1}$. For the default electron abundance 2.4×10^{-7} we used the expression in Oppenheimer & Dalgarno (1974); alternatively see McKee (1989). The default carbon isotopic ratio is $R_{12/13} = [^{12}\text{C}]/[^{13}\text{C}] = 60$. The entry for ‘M’ represents all heavy atoms with ionization potentials less than 10eV or so and the default is for strong depletion – the typical “low metals” case. Nitrogen was assumed to exist in the form of N_2 with a Solar $[\text{N}]/[\text{C}]$ ratio and carbon depletion in the model corresponds to the default value $X(\text{CO}) = 8 \times 10^{-5}$.

For He^+

$$dn(\text{He}^+)/dt = \zeta_{\text{He}}n(\text{He}) - n(\text{He}^+)n(\text{H}_2) \sum_j k_j X_j$$

where the fractional abundances of the reactants j are X_j and their reaction rate constants with He^+ are k_j (listed in Table 4). For He we take the local galactic disk abundance $[\text{He}]/[\text{H}] = 0.088$ (Balser 2006). The cosmic-ray ionization rate of He is $\zeta_{\text{He}} = 1.08 \zeta_{\text{H}_2}/2$ and $\zeta_{\text{H}_2} = 2 \times 10^{-17} \text{ s}^{-1}$. In general, direct recombination of atomic ions with ambient electrons is utterly insignificant in this context.

For $^{12}\text{C}^+$ and $^{13}\text{C}^+$

$$\begin{aligned} dn(^{12}\text{C}^+)/dt = & n(^{12}\text{CO})[n(^{13}\text{C}^+)k_f + n(\text{He}^+)k_{\text{He-CO}}] \\ & - n(^{12}\text{C}^+)[n(^{13}\text{CO})k_r + n(\text{H}_2) \sum_j k_{j-\text{C}^+} X_j] \end{aligned}$$

$$dn(^{13}\text{C}^+)/dt = n(^{13}\text{CO})[n(^{12}\text{C}^+)k_r + n(\text{He}^+)k_{\text{He-CO}}]$$

$$-n(^{13}\text{C}^+)[n(^{12}\text{CO})k_f + n(\text{H}_2) \sum_j k_{j-\text{C}^+} X_j]$$

In each panel of Fig. 2 the relative abundance $X(^{12}\text{C}^+)$ is shown by a solid (black) line and $X(^{13}\text{C}^+) \times R_{12/13}$ (the red dashed line) has been scaled up by the inherent isotopic abundance so that the gap between the solid black and dashed red lines shows directly the extent to which ^{13}C is depleted in C^+ and in the gas outside CO. The effect is generally very large at 10 K, though still somewhat below $\exp(35/T_K)$. The lower right panel shows the effect of artificially increasing the strength of the fractionation reaction, illustrating that depletion of $^{13}\text{C}^+$ might be a factor two stronger if competing reactions were less important.

Although the important chemical effects should be incorporated in the default model, its ^{13}C depletion (a factor 15) is much stronger than is seen even in CCH (at most a factor 4) and substantial ^{13}C depletion persists at relatively high temperature (the upper left panel). Of course none of this is observed. Lowering the $\text{C}^+/^{13}\text{C}^+$ ratio can be accomplished ad hoc by assuming an undepleted metal abundance, by putting all the spare oxygen in a species like O_2 or OH that reacts rapidly with C^+ , or by increasing the rate at which C^+ recombines with H_2 (lower left). Perhaps the least ad hoc modification is the case of small $X(\text{CO})$ because CO will eventually deplete from the gas phase. This modification is basically the effect suggested by Watson (1977) and modelled by Liszt (1978).

C. Appendix C. Is carbon fractionation reversible after formation?

In the fractionation chemistry the ambient $^{13}\text{C}^+$ is depleted by a factor somewhat smaller than $\exp(35 \text{ K}/T_K)$ corresponding to the binding energy difference in CO. In principle, if another molecule's chemistry was dominated by a fractionation reaction like that of C^+ and CO, with an energy defect comparable to 35 K and an abundance much less than that of C^+ (which itself is not large) so that the gas contains sufficient amounts of ^{13}C , that molecule's complement of ^{13}C could

be restored to a degree approaching the abundance ratio inherent in the gas, $R_{12/13}$. At present it is not possible to demonstrate that such in situ fractionation after formation occurs for any species beside CO: species either react chemically with C^+ to form other species or they react too frequently with other things beside C^+ , with the added complication that the rate constants of the required fractionation reactions are still unknown even 35 years since the importance of the CO fractionation reaction was established. CS is in fact one of the better chemical candidates, with an energy difference between CS and ^{13}CS of 26.3 K, but the fractionation reaction with C^+ has never been measured.

REFERENCES

- Bally, J. & Langer, W. D. 1982, *ApJ*, 255, 143
- Balser, D. S. 2006, *Astron. J.*, 132, 2326
- Bensch, F., Leuenhagen, U., Stutzki, J., & Schieder, R. 2003, *ApJ*, 591, 1013
- Boger, G. I. & Sternberg, A. 2006, *ApJ*, 645, 314
- Boland, W. & de Jong, T. 1982, *ApJ*, 261, 110
- Burgh, E. B., France, K., & McCandliss, S. R. 2007, *ApJ*, 658, 446
- Cambr sy, L. 1999, *A&A*, 345, 965
- Charnley, S. B. & Markwick, A. J. 2003, *A&A*, 399, 583
- Crovisier, J., Biver, N., Bockel e-Morvan, D., Boissier, J., Colom, P., & Lis, D. C. 2009, *Earth Moon and Planets*, 105, 267
- Flower, D. R., Le Bourlot, J., Pineau Des Forets, G., , & Roueff, E. 1994, *A&A*, 282, 225
- Frerking, M. A., Keene, J., Blake, G. A., & Phillips, T. G. 1989, *ApJ*, 344, 311
- Furuya, K., Aikawa, Y., Sakai, N., & Yamamoto, S. 2011, *ApJ*, 731, 38
- Gerin, M., Foss , D., & Roueff, E. 2003, in *SFChem 2002: Chemistry as a Diagnostic of Star Formation*, proceedings of a conference held August 21-23, 2002 at University of Waterloo, Waterloo, Ontario, Canada N2L 3G1., ed. C. L. Curry & M. Fich, 171–175
- Goldsmith, P. F., Heyer, M., Narayanan, G., Snell, R., Li, D., & Brunt, C. 2008, *ApJ*, 680, 428
- Hartogh, P., Lis, D. C., Bockel e-Morvan, D., de Val-Borro, M., Biver, N., K ppers, M., Emprechtinger, M., Bergin, E. A., Crovisier, J., Rengel, M., Moreno, R., Szutowicz, S., & Blake, G. A. 2011, *Nature*, 478, 218

- Langer, W. D., Graedel, T. E., Frerking, M. A., & Armentrout, P. B. 1984, *ApJ*, 277, 581
- Langer, W. D. & Penzias, A. A. 1993, *ApJ*, 408, 539
- Lepp, S., Dalgarno, A., van Dishoeck, E. F., & Black, J. H. 1988, *ApJ*, 329, 418
- Lis, D. C., Wootten, A., Gerin, M., & Roueff, E. 2010, *ApJ*, 710, L49
- Liszt, H. S. 1978, *ApJ*, 222, 484
- . 2007, *A&A*, 461, 205
- . 2009, *A&A*, 508, 783
- Liszt, H. S. & Lucas, R. 1998, *A&A*, 339, 561
- Lucas, R. & Liszt, H. 1998, *A&A*, 337, 246
- Maezawa, H., Ikeda, M., Ito, T., Saito, G., Sekimoto, Y., Yamamoto, S., Tatematsu, K., Arikawa, Y., Aso, Y., Noguchi, T., Shi, S., Miyazawa, K., Saito, S., Ozeki, H., Fujiwara, H., Ohishi, M., & Inatani, J. 1999, *ApJ*, 524, L129
- Martín, S., Aladro, R., Martín-Pintado, J., & Mauersberger, R. 2010, *A&A*, 522, A62+
- McKee, C. F. 1989, *ApJ*, 345, 782
- Milam, S. N., Savage, C., Brewster, M. A., Ziurys, L. M., & Wyckoff, S. 2005, *ApJ*, 634, 1126
- Mumma, M. J. & Charnley, S. B. 2011, *Ann. Rev. Astrophys. Astron.*, 49, 471
- Ohishi, M., Irvine, W., & Kaifu, N. 1992, in *Astrochemistry of cosmic phenomena: proceedings of the 150th Symposium of the International Astronomical Union, held at Campos do Jordao, Sao Paulo, Brazil, August 5-9, 1991*. Dordrecht: Kluwer, ed. P. D. Singh, 171–172
- Oppenheimer, M. & Dalgarno, A. 1974, *ApJ*, 192, 29

- Padovani, M., Walmsley, C. M., Tafalla, M., Hily-Blant, P., & Pineau Des Forêts, G. 2011, *A&A*, 534, A77
- Phillips, T. G. & Huggins, P. J. 1981, *ApJ*, 251, 533
- Pineda, J. L., Goldsmith, P. F., Chapman, N., Snell, R. L., Li, D., Cambrésy, L., & Brunt, C. 2010, *ApJ*, 721, 686
- Prasad, S. S. & Tarafdar, S. P. 1983, *ApJ*, 267, 603
- Pratap, P., Dickens, J. E., Snell, R. L., Miralles, M. P., Bergin, E. A., Irvine, W. M., & Schloerb, F. P. 1997, *ApJ*, 486, 862
- Sakai, N., Ikeda, M., Morita, M., Sakai, T., Takano, S., Osamura, Y., & Yamamoto, S. 2007, *ApJ*, 663, 1174
- Sakai, N., Saruwatari, O., Sakai, T., Takano, S., & Yamamoto, S. 2010, *A&A*, 512, A31+
- Sheffer, Y., Rogers, M., Federman, S. R., Abel, N. P., Gredel, R., Lambert, D. L., & Shaw, G. 2008, *ApJ*, 687, 1075
- Smith, D. & Adams, N. G. 1980, *ApJ*, 242, 424
- Smith, R. L., Pontoppidan, K. M., Young, E. D., & Morris, M. R. 2011, *Meteoritics and Planetary Science Supplement*, 74, 5406
- Sonnentrucker, P., Welty, D. E., Thorburn, J. A., & York, D. G. 2007, *Astrophys. J., Suppl. Ser.*, 168, 58
- Sternberg, A., Dalgarno, A., & Lepp, S. 1987, *ApJ*, 320, 676
- Takano, S., Masuda, A., Hirahara, Y., Suzuki, H., Ohishi, M., Ishikawa, S., Kaifu, N., Kasai, Y., Kawaguchi, K., & Wilson, T. L. 1998, *A&A*, 329, 1156

- Tercero, B., Cernicharo, J., Pardo, J. R., & Goicoechea, J. R. 2010, *A&A*, 517, A96+
- van der Tak, F. F. S., Müller, H. S. P., Harding, M. E., & Gauss, J. 2009, *A&A*, 507, 347
- Visser, R., van Dishoeck, E. F., & Black, J. H. 2009, *A&A*, 503, 323
- Wakelam, V. & Herbst, E. 2008, *ApJ*, 680, 371
- Wakelam, V., Herbst, E., Selsis, F., & Massacrier, G. 2006, *A&A*, 459, 813
- Wannier, P. G. 1980, *Ann. Rev. Astrophys. Astron.*, 18, 399
- Watson, W. D. 1977, in *Astrophysics and Space Science Library*, Vol. 67, CNO Isotopes in Astrophysics, ed. J. Audouze, 105–114
- Watson, W. D., Anicich, V. G., & Huntress, W. T., J. 1976, *ApJ*, 205, L165
- Willacy, K., Langer, W. D., & Allen, M. 2002, *ApJ*, 573, L119
- Wilson, T. L. 1999, *Rep. Prog. Phys.*, 62, 143
- Wilson, T. L., Mauersberger, R., Langer, W. D., Glassgold, A. E., & Wilson, R. W. 1992, *A&A*, 262, 248
- Wolfire, M. G., Tielens, A. G. G. M., Hollenbach, D., & Kaufman, M. J. 2008, *ApJ*, 680, 384
- Woodall, J., Agúndez, M., Markwick-Kemper, A. J., & Millar, T. J. 2007, *A&A*, 466, 1197
- Woods, P. M. & Willacy, K. 2009, *ApJ*, 693, 1360
- Xie, T., Allen, M., & Langer, W. D. 1995, *ApJ*, 440, 674

Table 1: Species, line frequencies and integrated line temperatures^a

Species	Frequency	Cyano Pk	L1527	NH ₃ Pk
	MHz	K-km s ⁻¹	K-km s ⁻¹	K-km s ⁻¹
HNC	90663.56	1.597(0.020)	1.850(0.040)	2.550(0.020)
HN ¹³ C	87090.85 ^b	0.551(0.023)	0.263(0.022)	0.650(0.026)
H ¹⁵ NC	88865.69	0.120(0.016)	0.055(0.015)	0.086(0.016)
CS	97980.95	0.980(0.011)	1.495(0.023)	1.685(0.010)
C ³⁴ S	96412.95	0.362(0.014)	0.116(0.009)	0.341(0.005)
¹³ CS	92494.27	0.121(0.008)	0.045(0.007)	0.100(0.008)
H ₂ CS	103040.28	0.483(0.012)	0.102(0.019)	0.272(0.011)
H ₂ C ³⁴ S	101284.40	0.0218(0.0044)		
H ₂ ¹³ CS	99077.84	0.0063(0.0016)		

^a Table entries are $\int T_R^* dv$ quantities in parentheses are 1σ uncertainty

^b For details of the HN¹³C spectrum see van der Tak et al. (2009)

Table 2: Integrated temperature and implied isotopologic ratios

Species	Cyano Pk	L1527	NH ₃ Pk
W(HN ¹³ C)/W(H ¹⁵ NC)	4.59(0.64)	4.78(1.36)	7.56(1.44)
N(HNC)/N(HN ¹³ C) ^a	54(8)..72(10)	52(15)..69(20)	33(6)..44(8)
N(HNC)/N(HN ¹³ C) ^b	43(6)..57(9)		
W(¹³ CS)/W(C ³⁴ S)	0.334(0.024)	0.385(0.066)	0.293 (0.028)
N(CS)/N(¹³ CS) ^c	68(5)	59(10)	77(7)
N(CS)/N(¹³ CS) ^d	71(5)		
W(H ₂ CS)/W(H ₂ C ³⁴ S)	22.9(4.2)		
W(H ₂ ¹³ CS)/W(H ₂ C ³⁴ S)	0.289(0.094)		
N(H ₂ CS)/N(H ₂ ¹³ CS) ^e	79(26)		

^a for N(HNC)/N(H¹⁵NC) = 250..330 and $\tau = 0$ in the HN¹³C line

^b for N(HNC)/N(H¹⁵NC) = 250..330 and $\tau = 0.6$ in the HN¹³C line.

^c for N(CS)/N(C³⁴S) = 22.7 and $\tau = 0$ in the C³⁴S line

^d for N(CS)/N(C³⁴S) = 22.7 and $\tau = 0.15$ in the C³⁴S line

^e for N(H₂CS)/N(H₂C³⁴S) = 22.7 and $\tau = 0$ in the H₂C³⁴S line.

Table 3: Other measured and inferred $^{12}\text{C}/^{13}\text{C}$ ratios^a

Species	Cyano Pk	1521E	L1527	NH ₃	ref
CCH/ ^{13}CCH	> 250 ^b		> 135 ^c		1
CCH/ C^{13}CH	> 170 ^b		> 80 ^c		1
CC ³⁴ S/ ^{13}CCS	230(43)	>130			2
CC ³⁴ S/ C^{13}CS	54(2)	51(4)			2
C ₃ ³⁴ S/ $^{13}\text{CCCS}$	> 191	> 107			2
HC ₃ N/H $^{13}\text{CCCN}$	79(11)				3
HC ₃ N/HC ^{13}CCN	75(10)				3
HC ₃ N/HCC ^{13}CN	55(7)			45(6)	3

^a Lower limits are 3σ , rms in parentheses are 1σ

^b $\text{C}^{13}\text{CH}/^{13}\text{CCH} = 1.6 \pm 0.4(3\sigma)$

^c $\text{C}^{13}\text{CH}/^{13}\text{CCH} = 1.6 \pm 0.1(3\sigma)$

References: 1) Sakai et al. (2010)

2) Sakai et al. (2007)

3) Takano et al. (1998)

Table 4: reactants and their rate constants with He^+ and C^+

Reactant	Relative abundance	w/He^+ $\text{cm}^3 \text{ s}^{-1}$	w/C^+ $\text{cm}^3 \text{ s}^{-1}$
H_2	1	$7.2 \times 10^{-15} + 3.7 \times 10^{-14} \exp(-35/T_K)$	$4.0 \times 10^{-16} (300/T_K)^{0.20}$
CO	8.0×10^{-5}	1.6×10^{-9}	see A1
e	2.4×10^{-7}		$7.2 \times 10^{-12} (300/T_K)^{0.83a}$
M	3.4×10^{-7}	3.3×10^{-9}	1.5×10^{-9}
CH	1.0×10^{-7}	$1.6 \times 10^{-9} \sqrt{(300/T_K)}$	$3.8 \times 10^{-10} \sqrt{(300/T_K)}$
OH	3.0×10^{-7}	$1.0 \times 10^{-9} \sqrt{(300/T_K)}$	$7.7 \times 10^{-10} \sqrt{(300/T_K)}$
O_2	1.0×10^{-7}	1.0×10^{-9}	1.0×10^{-9}
H_2O	1.0×10^{-7}	$4.8 \times 10^{-10} \sqrt{(300/T_K)}$	$2.7 \times 10^{-9} \sqrt{(300/T_K)}$
N_2	1.2×10^{-5}	1.6×10^{-9}	

^a Wolfire et al. (2008), includes dielectronic recombination